ORIGINAL RESEARCH ARTICLE

The Interface Zone of Explosively Welded Titanium/Steel after Short-Term Heat Treatment

MARCIN SZMUL, KATARZYNA STAN-GLOWINSKA, MARTA JANUSZ-SKUZA, AGNIESZKA BIGOS, ANDRZEJ CHUDZIO, ZYGMUNT SZULC, and JOANNA WOJEWODA-BUDKA

This work presents a detailed description of a bonding zone of explosively welded Ti/steel clads subjected to stress relief annealing, applied in order to improve the plasticity of the final product. The typical joint formed by the welding process possesses a characteristic wavy interface with melted regions observed mainly at the crest regions of waves. The interface of Ti/steel clads before and after annealing was previously investigated mostly in respect to the melted regions. Here, a sharp interface between the waves was analyzed in detail. The obtained results indicate that the microstructure of a transition zone of that area is different along the width. After the heat treatment at 600 °C for 1.5 hours, titanium carbide (TiC) together with α-Fe phase forms at the interface in local areas of relatively wide interlayer (~ 1 μm), while for most of the sharp interface, a much thinner zone up to about 400 nm, formed by four sublayers containing intermetallic phase and carbides, is present. This confirms that carbon diffusion induced by applied heat treatment significantly influences the final microstructure of the Ti/steel interface zone. Side bending tests confirmed high plasticity of welds after applied heat treatment; however, the microhardness measurements indicated that the strengthening of the steel in the vicinity of the interface had not been removed completely.

https://doi.org/10.1007/s11661-021-06174-z

I. INTRODUCTION

FOR the process apparatus dedicated to work in a chemically aggressive environment, stainless steel may not always be used. In such cases, technically pure Ti or Ti alloys are used as the material of higher corrosion resistance than stainless steels. The economical solution to this problem comes down to the use of a non-alloy steel clad with Ti or Ti alloys. This combination of materials is difficult to obtain by conventional methods; however, it can be achieved using explosive welding technology. The typical wavy interface of explosively welded Ti/steel clad[1] is accompanied by highly deformed grains of joined materials near the interface zone, as well as the areas subjected to remelting (observed mainly at the crest regions of the waves), causing a decrease of plastic properties of the weld.[2] The improvement of plasticity can be obtained by applying stress relief annealing. However, this process can lead to the coarsening of the microstructure due to the recrystallization as well as formation of additional intermetallic phases localized at the interface, which deteriorates the mechanical properties of the obtained material.[3–5] Thus, these two processes must be well controlled in order to provide the balance in the properties of the final product. Usually, the optical microscopy and scanning electron microscopy (SEM) techniques are applied to analyze the changes of the microstructure of Ti/steel clads after each process step. According to the literature, this analysis is mainly focused on the studies of the melted regions. For example, Chu *et al.*[2] studied detailed characteristics of the melted regions present in the typical wavy structure using electron microscopy techniques. The authors found the presence of FeTi and Fe_2Ti phases within the mixing zones. Manikandan *et al.*[3] studied the relation between kinetic energy loss and microstructure of the interface zone in Ti/stainless steel explosively welded clads to determine the value of kinetic energy at which the formation of intermetallics could be fully avoided or reduced. Also, in this case, the studies of microstructure were focused solely on the intermetallics

MARCIN SZMUL is with the Institute of Metallurgy and Materials Science, Polish Academy of Sciences, 30-059 Cracow, Poland, and FAMET S.A., 47-225 Kedzierzyn-Kozle, Poland. KATARZYNA STAN-GLOWINSKA, MARTA JANUSZ-SKUZA, AGNIESZKA BIGOS, and JOANNA WOJEWODA-BUDKA are with the Institute of Metallurgy and Materials Science, Polish Academy of Sciences. Contact email: j.wojewoda@imim.pl ANDRZEJ CHUDZIO is with FAMET S.A. ZYGMUNT SZULC is with High Energy Technologies Works Explomet, 45-641 Opole, Poland.

Manuscript submitted July 6, 2020; accepted January 31, 2020.
Article published online March 6, 2021

present within the vortices (FeTi and Fe_2Ti) of the melted regions. There are only a few literature reports regarding a detailed study of the Ti/steel clad interface after explosive welding at the nanometer scale with the aim of transmission electron microscopy (TEM) presenting microstructure and phase composition details.[4,6,7] Among these few studies, significant differences in descriptions of microstructure can be found. Song *et al.*[7] found two components of different morphologies regarding the thin layer located at the Ti/steel interface. The dominant one, adjacent to steel, was composed of strongly deformed nanosize crystallites of intermetallics, while closer to the Ti, the intermetallic layer of 100 to 300 nm with well-defined grains up to 30 nm was identified. The authors do not give the precise answer regarding what type of intermetallics were there, as it was impossible to recognize them due to the strong distortion of the crystal lattice and methodological limitations. The chemical composition of the latter sublayer varied from 80 to 56 at.pct Ti and 20 to 44 at.pct Fe. However, the difficulties in resolving the selected area diffraction pattern caused by high distortion of the lattice made it impossible to identify the phase composition of this sublayer. The presence of a single layer composed of nanosized FeTi intermetallics was observed at the Ti/mild steel interface located at the crest of the wave and reported by Chu *et al.*[2] The transition zone was well defined by a map of element distribution collected *via* TEM by Wachowski *et al.*;[4] however, the thin lamella was probed the same as in the Reference 2 from the crest of the wave. The authors revealed that the transition zone between the joined plates contained a mixture of Ti, Fe, and an increased content of Mn. Later, they subjected the examined explosively welded Ti/carbon steel S355J2 + N clad to short-term heat treatment of 600 °C for 90 minutes. As a result of this stress relief annealing, the interface transformed to two sublayers: The first was located next to steel and was composed of Ti carbide grains of size below 1 μm, and the second was located closer to Ti and was a mixture of TiC and fine precipitates of α-Fe in the matrix of Ti. On the other hand, Guoyin *et al.*[6] examined the Ti/steel interface after additional heat treatment (540 °C for 3 hours) and found the presence of a thin interfacial layer of 0.2-μm thickness located far away from the vortex with the aim of TEM. However, observations allowed them only to speculate that the nanoscale layer may be of the amorphous structure. It was also found that both Fe and Ti were the constituents and additionally small grains of α-Ti were detected. Interesting results were reported by Prasanthi *et al.*[8] who demonstrated that the Ti Gr.2/mild steel interface zone after annealing was composed of fine needlelike features of Fe_2Ti phase coexisting with parent ferrite phase.

All of these works describe the formation of the transition layer at the Ti/steel interface and the presence of FeTi and Fe_2Ti intermetallic phases within the vortexes immediately after the EXW process or subsequent annealing. However, it should be emphasized that in these reports, various steel and Ti alloys have been applied and none of them describe the changes in the microstructure of the Ti/steel interface in various locations at the sharp interface between the waves formed due to EXW and followed by heat treatment. Therefore, the goal of this study is to provide detailed TEM analysis of the bonded zone of explosively welded Ti/steel at the micro- and nanoscale after explosive welding and short-term annealing between the waves in locations without visible remeltings during observations using scanning electron microscopy. Furthermore, the durability of the obtained clads will be verified by bending tests followed by microhardness measurements, both usually applied to investigate the mechanical properties of such welds.

II. EXPERIMENTAL

Two types of materials (Table I) were subjected to the EXW: steel SA516 Gr. 60 with a thickness of 14 mm (base plate) and Ti Ti Gr.1 with a thickness of 2 mm (flyer plate).

After the explosive welding, the clad plate (1230 mm × 2980 mm) was annealed at 600 °C for 1.5 hours and then straightened. This reflects the condition of the explosively welded sheets supplied to the industry for further operations (*e.g.*, bending or welding). After the straightening process, the samples were prepared for SEM investigations. A metallographic procedure optimal for the optical and SEM microscopy observations including grinding using the abrasive papers up to 7000 grit, followed by mechanical polishing with a 1:1 solution of colloidal silica suspension and hydrogen peroxide (30 pct), was used, which resulted in highly polished, mirrorlike surfaces. Subsequently, the microstructure of the samples was studied using the optical microscopy method (Leica). The samples' surfaces were etched for observations under the optical microscope in two solutions: first in 6 pct HF and then in a mixture of hydrofluoric and nitric acids in water. The unetched samples' surfaces were also examined with the scanning electron microscope FEI Quanta 3D FEG using the backscattered electrons (BSE) mode equipped with an energy-dispersive X-ray spectrometer to perform the element map distribution within the waves as well as chemical point analysis to determine the type of intermetallic phases present in the melted regions. After observations of the interface morphology and melted regions composition, the thin lamellas were prepared from two areas of the interface without visible remeltings using a focused ion beam (FIB) instrument (Quanta 2D, FEI). The microstructure of the obtained lamellas was examined using the FEI Tecnai G2 200 kV including bright-field and high-resolution mode, chemical analysis using EDS (EDAX), and electron diffraction for phase identification.

Microhardness tests were performed in a direction perpendicular to the plane of the welded joint (Innovatest Nexus 4504 hardness tester) with a distance between indentations equal to 0.15 mm. Side bending tests were performed using the ZD-40 universal testing machine for

Table I. Chemical Composition of the Initial Materials

Commercially Pure Titanium—ASTM B265 Grade 1						
Chemical Composition (Mass Pct)						
Element	C	H	O	N	Fe	Ti
Range						
Min	—	—	—	—	—	bal
Max	0.08	0.015	0.08	0.03	0.07	100
Measured value	0	0.001	0.05	0	0.03	bal

Steel SA 516 Gr. 60 MT						
Chemical Composition, Mass Percent						
Element	C	Mn	Si	P	S	Cu
Measured Value	0.15	1.1	0.22	0.014	0.003	0.014
Element	Ni	Cr	Mo	V	Ti	Al
Measured Value	0.05	0.02	0.005	0.005	0.002	0.042
Element	N	Nb	B	Fe	—	—
Measured Value	0.004	0.005	0.0005	bal	—	—

the specimens of dimensions 16 × 10 mm × 210 mm. The bending radius was 20 mm, the spacing between the supports was 70 mm, and the bending angle was 180 deg.

III. RESULTS AND DISCUSSION

A. *Microstructure of the Interface Region*

As Ti is characterized by the high reactivity with oxygen and nitrogen at elevated temperatures, the explosive welding (jetting phenomenon) serves as the optimal solution for its welding with steel. However, the extreme conditions of explosive welding and the differences in the physical properties of Ti and steel result in the presence of large residual stresses within the interface region, thus influencing the durability and the mechanical properties of the weld.[9] Therefore, the importance of the microstructure observations should not be omitted. The microstructure of the weld with a characteristic wavy interface obtained in this study is shown in Figures 1(a) and (b). The melted regions (an example is shown by the arrow in Figure 2(a)), where strong intermixing of the bonded materials took place as revealed by elemental map distribution (Figures 2(b) through (d)), are located on both sides of the wave crest mostly in wave vortexes surrounded by steel. They are, however, not that common in the examined weld. Cracks were observed in the vortex region resulting from the shrinkage of melt during the solidification without further propagation to the neighboring areas (Figure 2(a)). Based on the chemical point analysis, the composition inside the melted regions (such as one showed with arrow in Figure 2(a)) corresponded to the stoichiometry of FeTi and Fe_2Ti intermetallic phases, as was previously shown in References 1, 2, and 4. As a result of explosive welding, the area of the material near the bonding interface has highly deformed grains and is

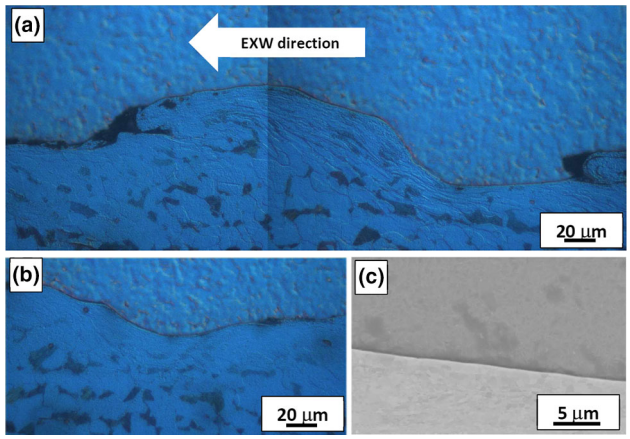

Fig. 1—Optical micrographs showing the microstructures of the Ti/steel interface: (*a*) a general view of the single wave; (*b*) an interface area between the waves (etched sample, Nomarski contrast); and (*c*) SEM (BSE) micrograph showing the part of the interface between the waves without visible areas of remelting.

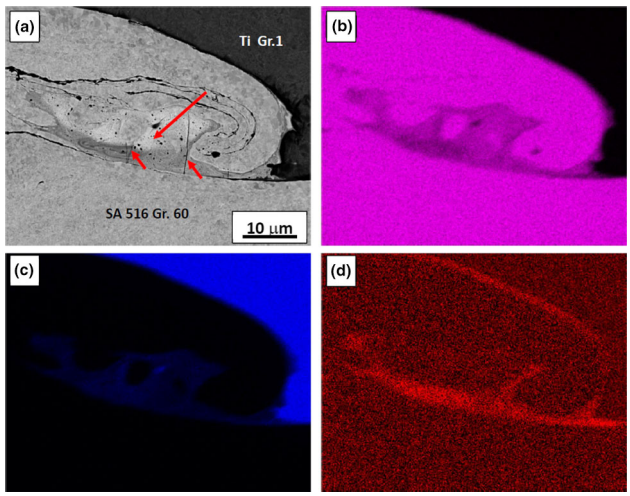

Fig. 2—SEM (BSE) micrograph showing the microstructure of the EXW joint in the wave region with visible areas of remelting (long arrow) and cracks (short arrows) (*a*) together with the distribution of elements in the selected area: (*b*) Fe (K), (*c*) Ti (K), and (*d*) C (K).

strongly strengthened, which can be especially observed for steel grains in Figure 1(a). These grains are elongated along the explosive direction, which is in agreement also with the previous reports (see, for example, Reference 6). The heat treatment was applied to reduce the internal stresses by inducing the recovery and recrystallization processes. As mentioned previously, such annealing can lead to the growth of the intermetallic phases and Ti carbides at the interface of the joined materials and, therefore, results in deterioration of the mechanical properties. Nevertheless, SEM/EDS examination did not reveal such a phenomenon under the applied annealing conditions in the areas located between the waves, as shown in Figure 1(c). Thus, further inspection of these interface regions was performed using TEM.

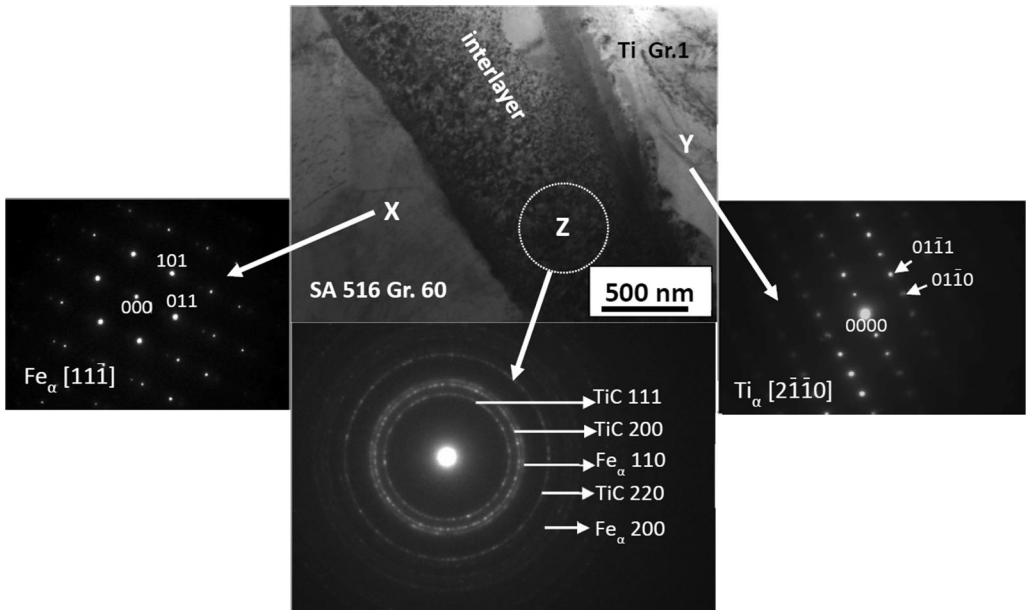

Fig. 3—TEM bright-field image showing the interface of the Ti/steel after the explosive welding process and heat treatment with electron diffraction taken from the interface region marked with the letter Z and selected area electron diffractions of steel (X) and Ti (Y).

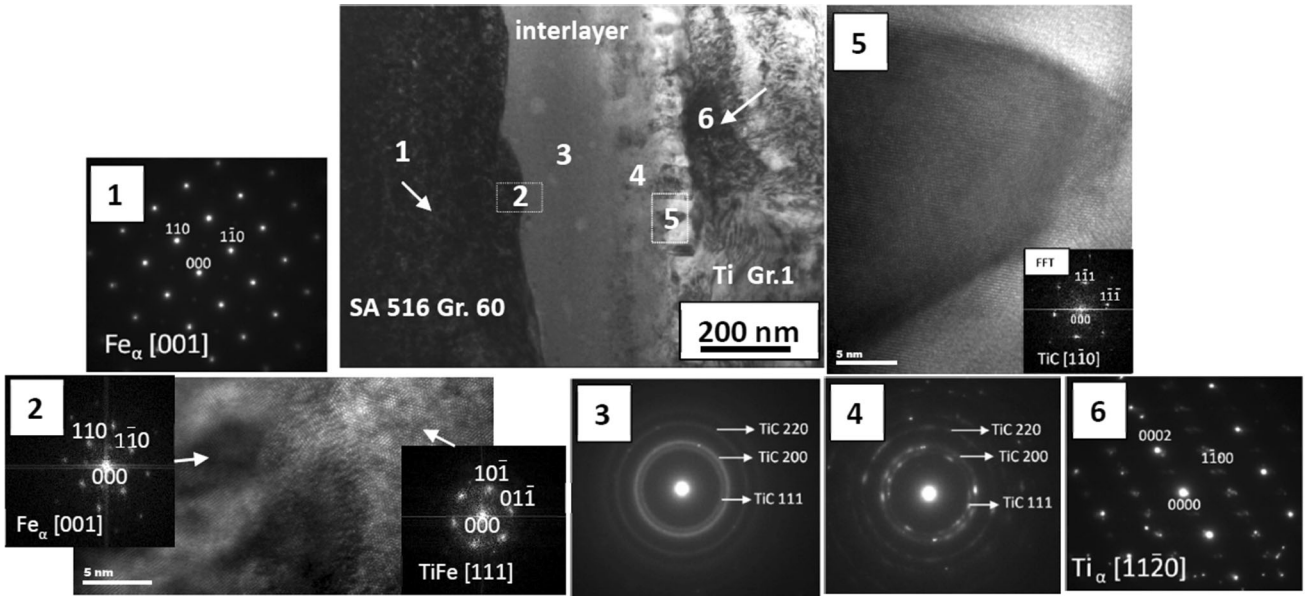

Fig. 4—TEM bright-field image showing the interface of the Ti/steel after the explosive welding process and heat treatment together with the electron diffractions taken from the layer(s) of the interface region marked with the numbers (3, 4) and high-resolution images (2, 5). The selected area electron diffractions were taken also from the surrounding materials: steel (1) and Ti (6).

Figures 3 and 4 show two sets of TEM data collected for the Ti/steel interface after EXW and heat treatment probed from two different places located between the waves. In the first region (Figure 3), surprisingly, the analyzed interface had a form of a remelted layer with thickness even up to 1 μm, which has broadened underneath the surface of the interface. It was composed of nanocrystalline TiC and α-Fe as evidenced by the electron diffraction shown in Figure 3 (zone marked "Z" in Figure 3). In contrast to this, in the second investigated area, the transition zone was only of 350 to 400 nm in thickness (Figure 4) and contained several sublayers. Their identification was done based on the electron diffractions and high-resolution images presented in Figure 4. The obtained patterns were indexed using crystallographic information found in the Inorganic Materials Database.[10] Next to the steel base material (SAED of α-Fe marked "1" in Figure 4), the layer of the FeTi intermetallic compound was identified with the cubic structure and lattice parameter of

a = 0.2972 nm (“2” in Figure 4). A subsequent layer with amorphous-like contrast was found to be composed of nanocrystals of TiC cubic phase (a = 0.4327), as confirmed by electron diffraction (“3” in Figure 4).

The next layer, when moving toward the Ti (α-Ti—SAED denoted “6” in Figure 4), was composed of the grains larger in size, with the diffraction contrast visible during bright-field observations. The electron diffraction for this region indicated that the layer also consisted of TiC particles (“4” in Figure 4). Finally, the last sublayer, located in the neighborhood of Ti, formed larger grains of TiC phase up to 100 nm in size. The example of a high-resolution image collected from one such grain is presented in Figure 4 (marked “5”). As is shown, the thickness of the remelted layer was not constant and varied along the joint depending from which place the lamella had been taken (Figure 3 *vs* Figure 4). However, it should be emphasized that Figure 4 can be considered as the representation of the Ti/steel interface region, as such type of interface prevails. Therefore, the scheme of the microstructure observed in the thinnest parts of the bonding zone can be schematically drawn, as shown in Figure 5. The performed analysis revealed that two phases are formed between α-Fe and α-Ti plates in this case: nanocrystalline FeTi intermetallic phase next to the steel base material and predominant nanocrystalline TiC carbide as a subsequent layer, which coarsens toward the α-Ti plate. This coarsening is not gradual but, rather, sharp interfaces could be distinguished between the various TiC sublayers. It should also be noticed that both types of formed phases, *i.e.*, FeTi intermetallic phase and carbide, have a cubic structure. The lattice mismatch between the structure of the base plate (α-Fe, a = 0.2866 nm) and the subsequently formed FeTi phase (a = 0.2978 nm) is ~ 4 pct, that between FeTi and cubic TiC (a = 0.43227 nm) is ~ 45 pct, and that between TiC and α-Ti (a = 0.29486 nm, c = 0.467 nm) is ~ 9 pct (if the c parameter of α-Ti is considered). Internal stresses induced by the lattice mismatch may also influence the properties of the bond formed between two such plates. Formation of carbides at the interface is generally related to the diffusion of carbon in the steel plate toward Ti being a result of the EXW process and subsequent heat treatment.[4,11] It was clearly evidenced

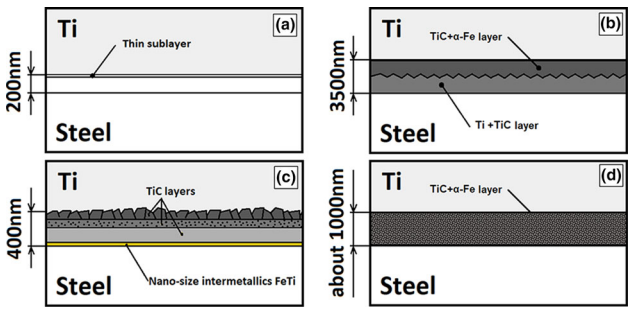

Fig. 5—Schemes of the interface microstructure after heat treatment taken from the literature, TEM observations reported in (*a*) Ref. 6 and (*b*) Ref. 4 compared to the ones obtained in this work from two localizations of the Ti/steel interface between the waves presented in (*c*) Fig. 4 and (*d*) Fig. 3.

by Haitao *et al.*[11] who examined explosively welded Ti/low-carbon steel (Q235B) being subjected to different rolling processes in the temperature range 700 to 850 °C. It is even more pronounced in the case of a sufficiently higher carbon content in the steel.[12] In the present study, the increased carbon concentration near the Fe/Ti interface was evidenced especially within the melted areas (see the map of element distribution presented in Figure 2(d)). Wachowski *et al.*,[4] who examined Ti Gr. 1/S355J2 + N steel after the same short heat treatment as the one used in this work (1.5 hours at 600 °C), also observed decarburization of the areas adjacent to the weld due to the diffusion of carbon toward Ti. In the analyzed area reported in Reference 4, fine α-Fe precipitates and TiC were found to grow toward the Ti direction with a thickness of approximately 3.5 μm. This is consistent with the observations made for the interface located between the waves with a higher width of remelted layer (up to 1 μm) found in the present study (Figure 3) but not with the thinner one (350 to 400 μm in width). The authors in Reference 4 indicated that two effects favor the carbide formation instead of intermetallic phases. First is the Ti/C ratio of raw materials. Nevertheless, the studies of the clad plates reported in Reference 4 concerned steel with a similar carbon content (0.19 wt pct in References 4 and 13) as that used in this work (0.16 wt pct), yet they gave different results despite the same heat treatment being applied. Thus, the differences in phase composition of the interlayer in the current work and that found in References 4 and 13 may be associated with the localization of the thin lamella investigated with TEM. In Reference 4, the lamella was cut from the crest of the wave, where a thin melted layer can be seen with SEM, whereas in Reference 13, there is no information on the localization of FIB lamella. It can be speculated whether the difference between the interface region shown in Figures 3 and 4 can be associated with the type of interface that has been examined—either Ti/ferrite or Ti/perlite. In the case of perlite (0.77 wt pct C), even short heat treatment can lead to diffusion of carbon, resulting in the formation of a microstructure such as the one presented in Figure 3. The second factor that influences the phase formation at the joint interface according to Reference 4 is the change in Gibbs free energy as a function of temperature, which is much lower for TiC compared to Fe_2Ti or FeTi phase in the temperature range related to the welding process and annealing. Studies of the interface formed directly after the EXW process did not reveal the formation of Ti carbides, while this phase is always observed to form after the additional heat treatment, which brings the system closer to equilibrium. The temperature increase during the welding process favors the remelting of the material and formation of the intermetallic phases especially at the crest of waves, where the highest local increase in temperature is expected. One can notice that the formation of intermetallic phases in this area is accompanied by the formation of carbides in the transition zone adjacent to it after annealing. In the area of the interface less affected by the increase in temperature, such as the area between the waves,

formation of intermetallics and subsequent diffusion of carbon (due to the heat treatment) will occur at a much smaller scale than in the previous case. In this case, the thin zone of intermetallics and carbides (after heat treatment) is expected, which is in agreement with our observations of interface microstructure. In the work of Jiang *et al.*,[5] Ti/steel explosive-rolling cladding plate was analyzed in terms of the influence of different heat treatments (650 to 950 °C for 60 minutes) on its microstructure and mechanical properties. In this case, the interface of the formed joint had a rather flat character and the parts and the interface were studied by TEM. It was found that Ti/steel explosive-rolling clad plate heated at 850 °C or below this temperature entails the formation of a TiC thin layer (300 nm) composed of TiC crystallites at the interface due to diffusion of carbon toward the Ti side and aggregation at the weld interface. Jiang *et al.*[5] reported that further diffusion of carbon into Ti was difficult due to the lower solubility of C in Ti alloy, while the low binding energy of TiC caused them to form on the interface, which suppressed the mutual diffusion of Fe and Ti, and the TiC was located next to the Ti side of the interface. Raising the rolling temperature to 950 °C resulted in the diffusion of Ti and Fe, and therefore, a layer of 200 to 300 nm composed of a Fe_2Ti and FeTi mixture of grains was formed along the interface of the Ti/steel clad plate. It was concluded that the temperature of 883 °C corresponding to the temperature of $\alpha \Leftrightarrow \beta$ transformation plays an important role in the formation and growth of the intermetallic compounds at the welded interface. This, in turn, influenced the shear strength of the weld, which decreased with the presence of FeTi-type intermetallics. Our study demonstrates that the temperature boundary (883 °C) pointed out in Reference 5 is not that sharp, and the FeTi compounds can be formed even after short-term annealing at 600 °C, as evidenced in the high-resolution image from TEM presented in Figure 4(c).

B. *Mechanical Tests*

In order to confirm the plastic properties of the weld after the applied heat treatment, the side bending tests comprising the elongation of 24 pct were performed followed by the observations of the tensile reference surface. The view of the sample after side bending is shown in Figure 6(a), where no cracks were observed in the macroscale (Figure 6(b)). Microstructural changes of samples subjected to plastic deformation were also examined with a scanning electron microscope. These observations (an example of such microstructure is presented in Figure 6(c)) allow exclusion of any material discontinuities, which confirms the high quality and plasticity of the weld after applied heat treatment. The microstructural observation results were similar for all tested samples, and the only crack-type discontinuities were observed within the volume of the melted regions (arrows in Figure 6(c)). This indicates the brittleness of the remelting zones due to the presence of intermetallic phases in a relatively large volume. Similar results, but with a different stress state, were obtained in References 8, 14, and 15, where also no crack propagation beyond the areas of remelting was observed.

The microhardness measurements were performed across the interface and included the tests of both base and clad plates at a given distance (up to 1.5 mm) from their interface. These measurements were performed across the interface avoiding a broad zone of the solidified melts, as this study is dedicated to the apparently sharp Ti/steel interface. The microhardness tests are the basic indicator of the effect of stress relief annealing influence on the reduction of the strengthening after the explosive welding process. In general, after the explosive welding process and near the weld, the materials are characterized by a highly deformed microstructure, which is associated with the phenomenon of strengthening and a decrease in plastic properties. Postcladding heat treatment allows leveling of the effects of strengthening and causes an increase of joint plasticity. Thus, it allows further plastic deformation of explosively welded materials, *e.g.*, bending, stamping, rolling, and welding, and therefore, it is a basic stage of the technological process of manufacturing equipment made of explosively welded materials. As shown in this work with the aim of TEM as a result of diffusion processes during the short heat treatment of Ti/clad steel, creation of undesirable brittle Fe_xTi_y and TiC phases takes place; however, this region of interest is localized at the interface with the thickness below 1 μm. It was expected that, as a result of recrystallization and recovery processes, the defected microstructure

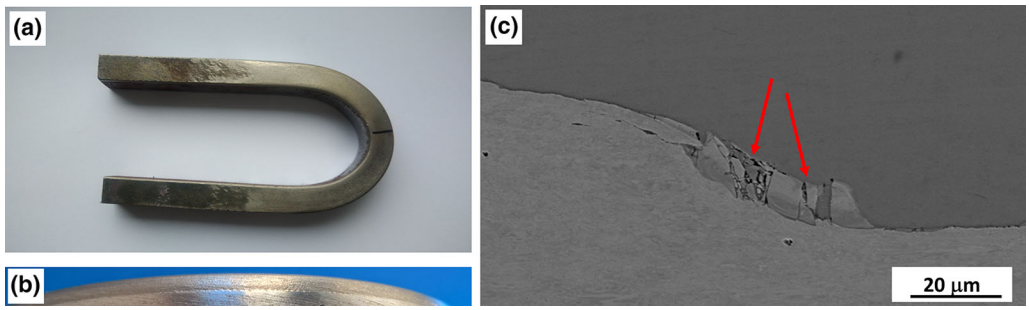

Fig. 6—Exemplary sample after the bending test: (*a*) a side view and (*b*) the surface after bending in the macroscale together with (*c*) the SEM image of the Ti/steel microstructure interface after the side bending test.

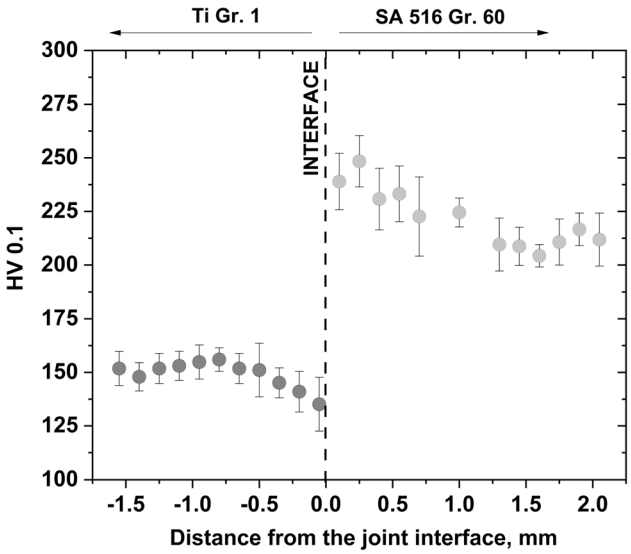

Fig. 7—Distribution of the microhardness values across the Ti/steel clad plate after heat treatment.

is rebuilt and the grains grow, which will affect the obtained microhardness values. Figure 7 shows the summary of the microhardness tests of the samples after applied heat treatment. Microhardness values are significantly lower for the clad material in comparison to the base material. These values vary in the range of 130 to 170 HV0.1 for Ti and 200 to 240 HV0.1 for steel. In the area close to the interface of the steel side, there is an increase in microhardness, pointing out that the strengthening after this heat treatment has not been completely removed. These values can be compared to those in Reference 4, where thicker Ti flyer plate has been applied (6 mm) in comparison to that used in this study (2 mm). However, the microhardness values for Ti Gr. 1 presented in the graph in Figure 7 are similar to these obtained in Reference 4. Additionally, at the Ti side in the vicinity of the interface, reduced microhardness values were observed, similar to those in Reference 4, where they were explained by the recovery, recrystallization, and loss of adiabatic shear bands in the microstructure.

IV. CONCLUSIONS

The interface zone created between Ti Gr. 1 and steel SA516 Gr. 60 due to the explosive welding followed by relatively short annealing comprising 1.5 hours at 600 °C was carefully analyzed with optical and electron microscopy techniques. This examination showed that the chemical composition of the melted regions corresponded mostly to FeTi and Fe_2Ti intermetallic phases. Particular interest was associated with the interface region located between the waves. A continuous remelted layer of 350–400 nm in thickness, in some locations reaching 1 μm thickness, is formed in the bonding zone located between the waves. Detailed TEM examination revealed that the microstructure changes with the thickness of this layer. The interface decorated with a thin layer is, in fact, composed of four sublayers, FeTi intermetallic (next to the steel) and three TiC layers of significantly various grain sizes up to 100 nm, while in the areas of the interface, where the melted region is significantly wider, the microstructure is composed solely of TiC and α-Fe. Formation of the observed carbides indicates that carbon diffusion plays a significant role in the formation of the interface zone formed due to the explosive welding followed even by relatively short-term annealing. Thus, carbon concentration in steel is an important factor in the designing microstructure of the interface of the obtained clad plate especially concerning the selection of the temperature of stress relief annealing. Additionally, due to the applied explosive welding process followed by heat treatment, an extremely thin layer of the brittle FeTi phase is present along the interface of the obtained plate. Despite this, the weld after heat treatment was characterized by high plasticity (elongation about 24 pct), which was confirmed during side bending tests, and the microhardness measurements show that the strengthening of the steel in the vicinity of the interface has not been removed completely.

ACKNOWLEDGMENTS

This work was financed by the Ministry of Science and Higher Education of Poland upon Decision Number 6/DW/2017/01/1 and the FAMET S.A. Company. SEM and TEM examination were performed within the accredited testing laboratories of the Institute of Metallurgy and Materials Science, Polish Academy of Sciences.

OPEN ACCESS

REFERENCES

1. N. Kahraman, B. Gülenç, and F. Findik: *J. Mater. Process. Technol.*, 2005, vol. 169, pp. 127–33.
2. Q. Chu, M. Zhang, J. Li, and C. Yan: *Mater. Sci. Eng. A*, 2017, vol. 689, pp. 323–31.
3. P. Manikandan, K. Hokamoto, A.A. Deribas, K. Raghukandan, and R. Tomoshige: *Mater. Trans.*, 2006, vol. 47, pp. 2049–55.
4. M. Wachowski, M. Gloc, T. Ślęzak, T. Płociński, and K.J. Kurzydłowski: *J. Mater. Eng. Perform.*, 2017, vol. 26, pp. 945–54.
5. H. Jiang, X. Yan, J. Liu, and X. Duan: *Trans. Nonferrous Met. Soc. China*, 2014, vol. 24, pp. 697–704.
6. Z. Guoyin, S. Xi, and Z. Jinghua: *Rare Met Mater. Eng.*, 2017, vol. 46 (4), pp. 906–11.
7. J. Song, A. Kostka, M. Veehmayer, and D. Raabe: *Mater. Sci. Eng. A*, 2011, vol. 528, pp. 2641–47.
8. T.N. Prasanthi, C.S. Ravikirana, and S. Saroja: *Mater. Des.*, 2016, vol. 93, pp. 180–93.
9. A. Karolczuk, H. Paul, Z. Szulc, K. Kluger, M. Najwer, and G. Kwiatkowski: *J. Mater. Eng. Perform.*, 2018, vol. 27, pp. 4571–81.
10. Xu. Yibin, Masayoshi. Yamazaki, and Pierre. Villars: *Jpn. J. Appl. Phys.*, 2011, vol. 50, p. 11.
11. J. Haitao, Y. Xiaoqian, L. Jixiong, D. Xiaoge, and Z. Shangwu: *Rare Met Mater. Eng.*, 2014, vol. 43 (11), pp. 2631–36.
12. T.N. Prasanthi, C. Sudha, P.K. Parida, A. Dasgupta, and S. Saroja: *Metall. Mater. Trans. A*, 2015, vol. 46A, pp. 1519–34.
13. M. Gloc, M. Wachowski, T. Plocinski, and K.J. Kurzydlowski: *J. Alloys Compd.*, 2016, vol. 671, pp. 446–51.
14. Q. Chu, X. Tong, S. Xu, M. Zhang, J. Ji, F. Yan, and C. Yan: *J. Mater. Eng. Perform.*, 2020, vol. 29, pp. 78–86.
15. J. Ning, L. Zhang, M. Xie, H. Yang, X. Yin, and J. Zhang: *J. Alloys Compd.*, 2017, vol. 698, pp. 835–51.